SOLDIER SYSTEM POWER SOURCES

FINAL PROJECT REPORT

CONTRACT # N00014-03-1-0952

31 July 2003 – 15 August 2006

Submitted to

Maj Alan Stocks
Office of Naval Research

Submitted by

Dr. Roger A. Dougal
Dr. Lijun Gao
Dept. of Electrical Engineering
University of South Carolina
Columbia, SC 29208

31 December 2006

TABLE OF CONTENTS

ABSTRACT

This work addressed five key issues related to effective use of electric energy by dismounted troops, working both at the individual level and at the squad level, with the fundamental goal of reducing the total mass of the electric power sources carried by a Marine in the Expeditionary Forces while still meeting all of his electric power demands. To achieve that goal, this work investigated the effectiveness of hybrid power sources composed variously of batteries, fuel cells, and super capacitors, it developed control algorithms for those hybrid power sources, it assessed the value of recovering energy from partially spent primary cells, it developed more-efficient methods of capturing energy from photovoltaic sources, and it developed simulation-based tools for planning the carriage of sufficient electric energy to power specific suites of equipment as necessary to accomplish specific missions.

INTRODUCTION

Soldier systems power sources were explored in a multidisciplinary and multidimensional effort that encompassed multiple aspects of the problem -- from understanding and improving individual power source components to integrating those components into effective systems, predicting the performance of those systems, and providing tools to best use those systems.

During this project, twenty-seven (27) journal and conference papers were published and one invention disclosure was filed. The publication list is detailed in Section 8. Papers [2, 21] focus on modeling of batteries and fuel cells. Papers [12, 15, 18, 24] describe the design and performance of fuel cell powered battery charging systems. Studies of hybrid fuel cell/ battery power sources are detailed in papers [3, 6, 8, 13, 14, 16, 17, 20, 25, 26] and hybrid battery/ultracapacitor power sources in papers [7, 22]. Papers [4, 5] describe the usage of secondary batteries as temporary energy repositories and the design of an automatic energy recovery system for partially spent batteries. Papers [1, 9, 10, 11, 19, 23] present study results on photovoltaic power systems. Finally, a preliminary patent on technology for optimally configuring solar power sources for mobile equipment has been disclosed and filed as described in [27] Because of the completeness of these papers, this report provides only an overview of the accomplishments. The full story on each can then be obtained from the corresponding publication(s). All the publications reported here were supported to some extent by this project (contract number N00014-03-1-0952) although some also inherited components from the prior project (Modeling of Power Systems for Marines -contract number N00014-00-1-0368) but were not reported on that prior project due to publication delays.

A simulation tool called "Battery Analyzer for Squad Level Mission Planning" was developed which considers power requirements of various equipment during missions and associated operational environments. The tool operates in conjunction with the Virtual Test Bed (VTB) software (which was used extensively in all aspects of this work) to specify battery carriage requirements that will maximize the energy available to each member of a squad without increasing the total battery count that has to be carried. In addition, it is used to evaluate alternative sources, e.g., fuel cells. Details are described in Section 7.

The work had four significant foci. The first was understanding and modeling of individual electrochemical power components, such as batteries, fuel cells, and ultracapacitors, etc. The second was design and assessment of hybrid power systems by integrating those components with/without necessary power electronics. The third was development of a power source evaluation tool that can be used to estimate the power requirements for any particular mission based on likely equipment use scenarios. The fourth was exergy minimization analysis that can be used to identify specific schemes for energy utilization that maximize the value of every watt-hour of energy carried while minimizing the risk of being caught without power when it is needed. As a result of these studies, we believe that we are poised to make significant improvements in the capabilities of solider power systems. Specific accomplishments of the studies include:

- Battery and fuel cell models
    - Dynamic battery models have been developed in the VTB, which are suitable for virtual-prototyping of battery involved power systems. Models account for nonlinear equilibrium potentials, rate- and temperature-dependencies, thermal effects and response to transient power demand. The models are based on publicly available data such as the manufacturers' data sheets. Model outputs agree both with manufacturer's data and with experimental results.
    - A system-level PEM fuel cell model has been formulated in the VTB, which accounts for the electrochemical voltage-current relationship, heat production, fuel and air consumption, temperature and pressure dependence, and estimated mass of the stack.
    - A DMFC model has been developed in the VTB. The model covers the physical aspects of the DMFC that most significantly impact its system level performance, including separate anode and cathode kinetics, mass transport losses, parasitic losses caused by methanol crossover, and heat losses due to convection and

water vaporization. The model also includes and represents the transient characteristics of the voltage and temperature.

- An advanced programmable load model was developed. The time dependent load characteristics are described by a look up table in the user-friendly form of an Excel spread sheet. When configured for natural coupling to a power network, this model functions as a voltage (or pressure, speed, etc.), current (or mass flow, torque, etc.), resistive, or power load. When configured for signal coupling, this model can control signal dependent source models.
- Reference mission scenarios and test beds. A probabilistic load profile generator was developed in MS Excel, which allows a user to define particular suites of equipment and usage scenarios for that equipment, that can then be used to evaluate the efficacy of arbitrary power sources.
- Hybrid power systems
  - A zinc-air battery/ lithium ion battery hybrid power source was studied by using simulation models and also by testing on actual hardware. The performance of the hybrid was compared to that of a lithium ion battery to demonstrate the improvement in performance on both specific power and specific energy.
  - An actively controlled battery/ ultracapacitor hybrid power source was investigated through both simulations and experimental tests. A DC-DC power converter actively controlled the flow of power between the battery, the ultracapacitor, and the load. A specific example of the hybrid that was built from two size 18650 lithium-ion cells and two 100-F ultracapacitors achieved a peak power of 132W, which is three-times larger than that of a corresponding passive hybrid power source (without a power converter), and a seven times better than the lithium-ion cells alone.
  - Two configurations of an actively controlled fuel cell/ battery hybrid system were studied with special attention to the peak power enhancement, control design, and power losses in the DC-DC converter. Both of the defined configurations were built using a 35 W polymer electrolyte membrane (PEM) fuel cell, an 8-cell lithium-ion battery pack, and a high-efficiency power converter. Both configurations yielded a peak power output of 135 W, about 4 times as high as the fuel cell alone could supply, with only a slight (13%) increase of weight.

- A fuel cell powered battery charging station was investigated by simulation and experiments and two control strategies were developed. The first control strategy adjusted the charging currents of the batteries being simultaneously charged in real-time according to the estimated state-of-charge (SOC) of each cell, which was obtained by estimating the battery open-circuit voltage with current correction and linearly fitting between the open-circuit voltage and the state-of-charge. The second is a synergetic control strategy. A practical synergetic controller to coordinate pulse current charging of the battery was synthesized and discussed. It provides asymptotic stability with respect to the required operating modes, invariance to load variations, and robustness to variation of the input and converter parameters.

- Exergy minimization
  - An intelligent scheduling of the use of specific batteries in specific equipment was designed.
  - Energy reclamation from partially depleted primary batteries, using secondary battery cells as temporary energy repositories, was studied in simulations.
  - An automatic energy optimization system was studied in simulations. It shows the feasibility of recovering energy from partially depleted primary batteries and consolidating it into one or more secondary batteries.

- Photovoltaic Power System
  - A state space approach to the design of a maximum power point (MPP) tracking system for photovoltaic energy conversion was presented and simulated.
  - An optimum configuration of cell connections to maximize the power generated by a solar array was investigated. The study found that, under complex irradiance conditions, the power generation capability of a solar array using the proposed configuration is enhanced by a factor of 2 without extra component costs. In addition, tracking at the maximum power point is significantly simplified. By controlling the solar array terminal voltage to follow prescribed values, the power generation is maximized; thus, the complexity of hardware implementation is reduced and the control stability is enhanced.

This report is arranged as follows: Sections 2 and 3, respectively, describe the development of component models and reference mission scenarios. Section 4 details the studies of hybridization schemes including battery/ battery hybrids, fuel cell/ battery hybrids, battery/ ultracapacitor hybrids, and fuel cell powered battery chargers. Section 5 describes the exergy minimization analysis and Section 6 presents the efficacy study of photovoltaic power systems. Finally, in Sections 7 and 8, we describe the project deliverables and the publications that resulted from this work. The appendices contain related model help files and copies of the publications. Executable software is provided on a separate CD.

MODELS OF POWER SOURCE COMPONENTS

A set of simulation models for standard power sources of interest to the Marine Corps has been developed for the Virtual Test Bed environment: 1) models of battery types include Lithium ion, Li-SO2, Li-MnO2, Zinc-air, and Alkaline; 2) models of fuel cell types include PEM and DMFC.

MODELING OF BATTERIES

A generic formulation for system-level models of lithium ion batteries was developed. The formulation accounts for nonlinear equilibrium potentials, rate- and temperature-dependencies, thermal effects and response to transient power demand. To fit all of these data, the electrical model has three components: 1) an equilibrium potential E, 2) an internal resistance having two components R_1 and R_2, and 3) and an effective capacitance that represents localized storage of chemical energy within the porous electrodes. The thermal model has lumped heat capacity, heat source, and thermal resistance to the ambient. The schematic of the electrical equivalent is shown in Fig. 2.1.

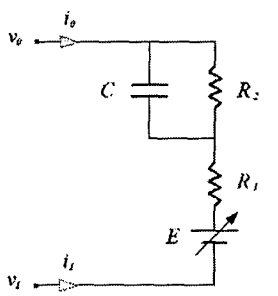

Fig. 2.1. Schematic of electrical model of lithium ion battery.

The procedure for developing the model involves first establishing one typical curve of battery voltage verses the depth of discharge as the reference curve. To yield the highest overall

accuracy, this reference curve should lie near the median expected operating current, usually the 1-C or 0.5-C rate. The equilibrium potential as a function of the state of discharge was then found by excluding the ohmic losses. Secondly, the discharge rate (i.e. the current) for the reference curve was chosen as the reference rate. Thirdly, the temperature for the reference curve was chosen as the reference temperature. The dependence of the state of discharge on temperature was accounted for by a temperature factor, which has value unity for the reference curve. In the 4th and final step, a temperature-dependent potential correction term was used to compensate for the variation of equilibrium potential that is induced by temperature changes at the reference rate. Figs. 2.2 and 2.3 show the resulting rate dependence of the potential and temperature dependent characteristics. It can be seen that the model outputs matches the manufacturer's data well.

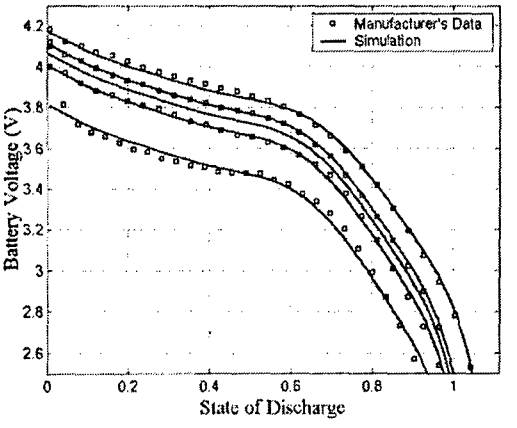

Fig. 2.2. Rate dependence of the battery voltage for currents of (from top to bottom) 0.28 A, 0.7 A, 1.0 A, 1.4 A, and 2.8 A at a constant temperature of 23 C.

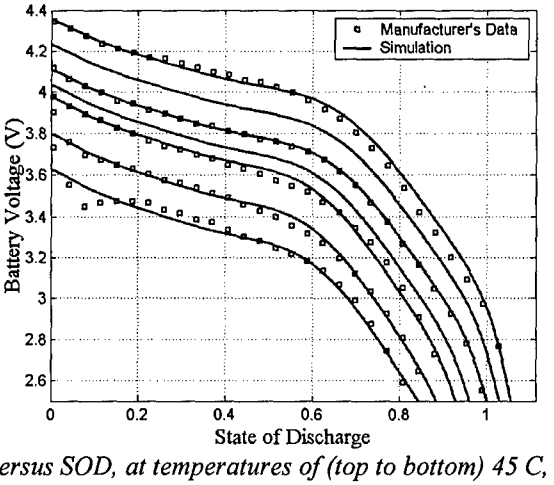

Fig. 2.3. Battery voltage versus SOD, at temperatures of (top to bottom) 45 C, 34 C, 23 C, 10 C, 0 C, -10 C, and -20 C. The discharge rate is 0.7 A.

This modeling method was extended and modified to the other types of battery models including Li-SO_2 Battery (BA5590U15V), Li-SO_2 Battery (BA5800U6V), Alkaline AA/AAA battery, and Generic battery.

MODELING OF FUEL CELLS

Polymer Electrolyte Membrane (PEM) fuel cell model

A polymer electrolyte membrane fuel cell model was developed. It includes the electro-chemical voltage-current relationship, heat production, fuel and air consumption, temperature and pressure dependence, and estimated mass of the stack. The model equations were derived from peer reviewed academic journals, internal studies, and texts on the subject of fuel cells.

Fig. 2.4 shows a test schematic that can be used to evaluate parameter settings, and sample results. Note that the simulation results are indistinguishable from the calculated values. This model is valid only when positive current is sourced by the fuel cell, and for feedstock pressures and temperatures within the ranges of 7.4-30 PSIG, and –10 to 60 Celsius respectively.

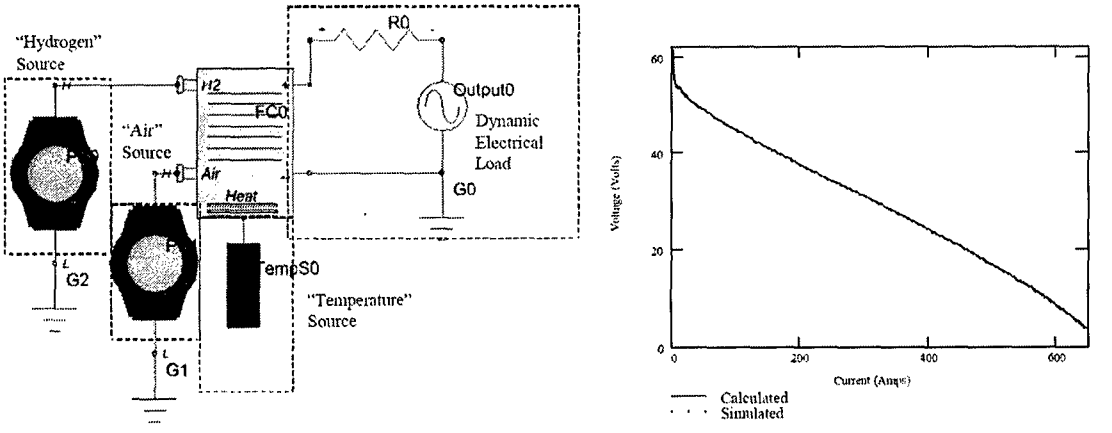

Fig. 2.4. VTB Schematic used to evaluate parameter settings, and sample results.

Direct Methanol Fuel Cell (DMFC) model

A system level model of a direct methanol fuel cell (DMFC) stack was built. The model covers the physical aspects of the DMFC that most significantly impact its system level performance, including separate anode and cathode kinetics, mass transport losses, parasitic losses caused by methanol crossover, and heat losses due to convection and water vaporization. The model also represents the transient characteristics of the voltage and temperature. The stack performance is highly dependent on operating conditions such as temperature and reactant concentrations, and so the model, like the real fuel cell, will perform effectively only if the stack temperature is adequately maintained and sufficient quantities of oxygen and methanol are supplied.

The model was derived on a region by region basis, with different regions connected together at boundaries where natural conservation laws are enforced. The physical processes within each region were modeled independently. The fuel cell model represents the effects of flow channels on the anode and cathode sides of the bipolar plates, anode and cathode catalyst layers where

the electrochemical reactions occur, backing layers for transporting reactants from the flow channels to the catalyst surfaces, and bipolar plates that store and transfer heat. The physical equations for the stack were derived under the assumption that each cell in the stack behaves the same as each other cell in the stack, and that each unit area of any cell behaves the same as any other unit area, so that the stack performance scales linearly with area and number of cells. The model does not account for variations between cells, but multiple instances of the stack model can be connected in series or parallel in order to represent cell-to-cell variations in voltage, fluid pressures, fluid concentrations, temperature, and so forth.

The validity of the DMFC model was demonstrated using a high level comparison between simulated results and results determined experimentally in a laboratory environment. Fig. 2.5 shows the system configuration used to validate the DMFC model. Fig. 2.6 illustrates the steady state voltage responses at various inlet methanol concentrations for a stack at a constant temperature of 70°C. Overall, the numerical data matches the experimental data well. It is noted that the model accuracy can be improved if more experimental data is collected over a larger set of methanol concentrations.

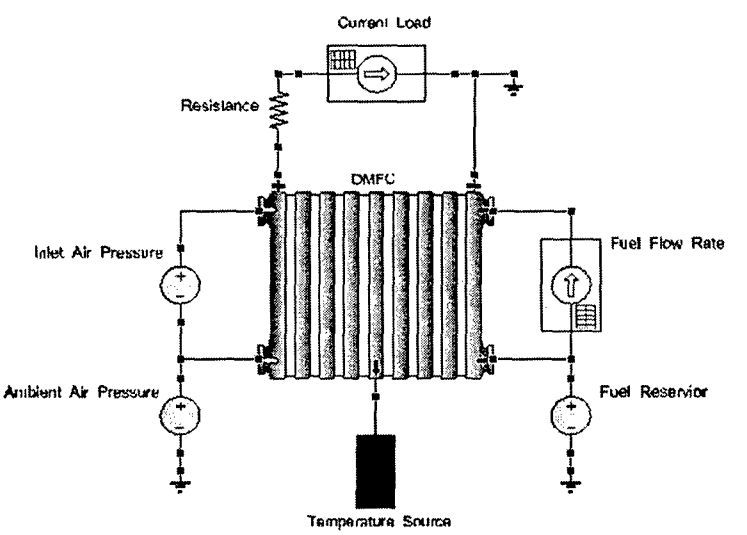

Fig. 2.5. System configuration used to validate the DMFC model.

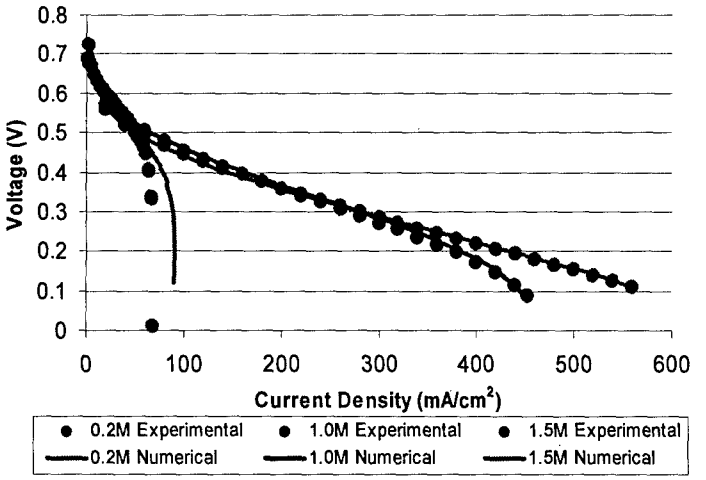

Fig. 2.6. Steady state voltage responses at various inlet methanol concentrations for a stack at a constant temperature of 70°C.

REFERENCE MISSION SCENARIOS AND TEST BEDS

MODELS FOR SOLDIER SYSTEM EQUIPMENT

An advanced programmable load model for use in the VTB was developed. The load is time dependent, and it is characterized by a look up table in an Excel spread sheet. When natural coupled, this model functions in any of four modes: either as a voltage (pressure, speed, etc.) source, a current (mass flow, torque, etc.) source, a dissipative (resistive) load, or as a power load. When signal coupled, this model functions as a signal generator that can control signal-dependent source models. By referencing different Excel spread sheets, the model can be used to represent different pieces of user defined soldier system equipment.

ADVANCED PROBABILISTIC LOAD PROFILE GENERATOR MODEL

An advanced probabilistic load profile generator model was built. The program uses a probabilistic algorithm to generate load profiles for a set of items each time the program is executed. The items in the set are defined individually, with each item having its own set of operating modes based on corresponding usage statistics. For example, as shown in Fig. 3.1, the worksheet named "Item 1" defines the operation statistics of the Item-1. In this example, the item has three operating modes: standby, active, and peak. Modes are listed under the "Mode Name" header and the number of modes is not limited. The next two columns specify the probability that each mode occurs and the load value of the item when the mode occurs. The item has a 70% chance of being in the standby mode, and when it is in the standby mode, the item draws 1W of

power. The remaining two columns specify the maximum and minimum duration that the item will operate in the corresponding mode. These limits are optional and can be left blank.

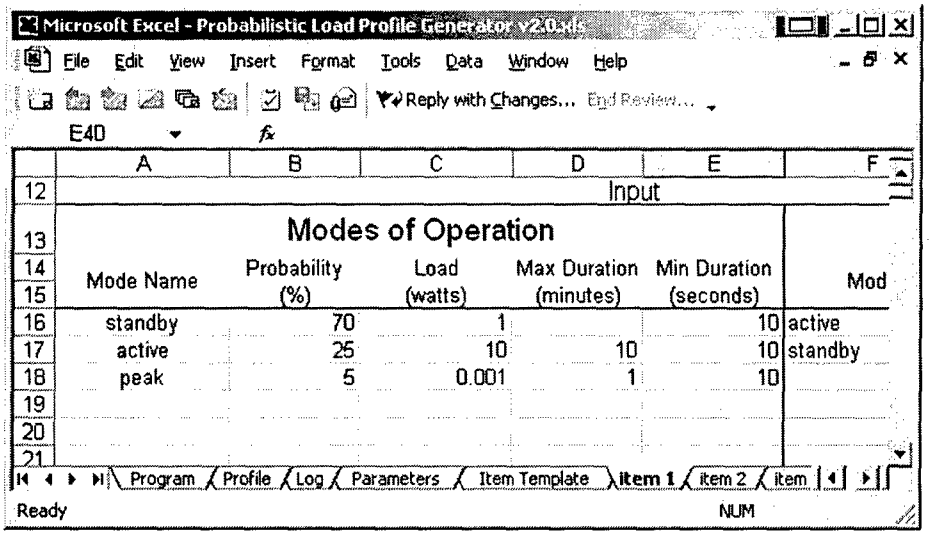

Fig. 3.1. Definition of each item.

When the program is executed, a profile for each item is generated individually. After every item is processed, the profiles are merged together on a single worksheet. Users can now either save a load profile for each item individually, or save the combined load profile for this set of items. An example of generated load profile is given in Fig. 3.2. It is noted that, time (in seconds) is entered in column "A" of the Excel spreadsheet, and the corresponding load values are entered in column "B". This example uses row 1 to identify the load profile as an "example input spreadsheet for the Advanced Programmable Load model." The third row is used for labeling the column headings 'Time(s)' and 'Load(W)'. Additional documentation about this model is available in the model help file.

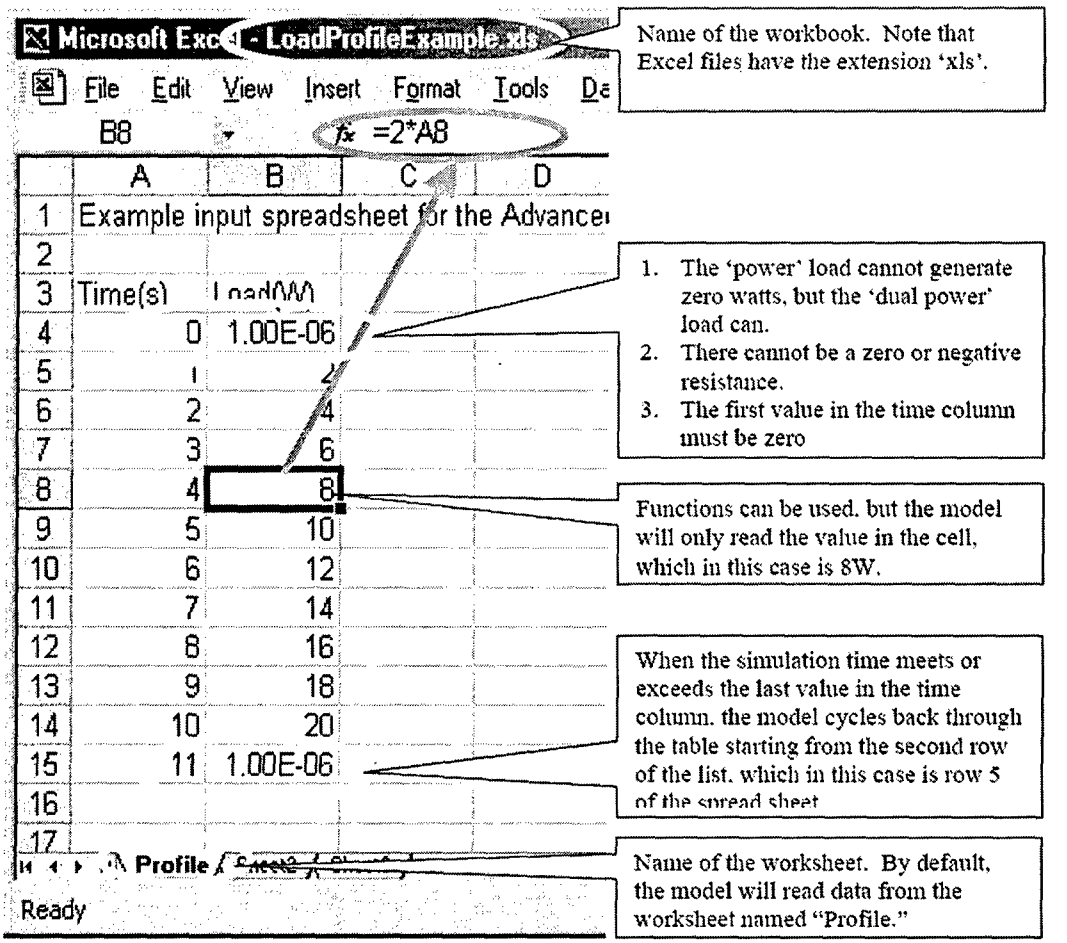

Fig. 3.2. The load profile example written in Excel.

EFFECTIVENESS OF HYBRIDIZATION SCHEMES

ZINC-AIR BATTERY - LITHIUM BATTERY HYBRID POWER SOURCE

The performance of a hybrid system comprising a zinc-air battery and a lithium-ion battery was explored by using simulation models and also by testing on actual hardware. The hybrid has an energy density higher than that of a lithium-ion battery (comparable to that of a zinc-air battery) and a peak power capacity larger than that of a zinc-air battery (comparable to that of a lithium-ion battery). A behavioral model of a zinc-air battery was created based on manufacturers' data sheets. In the experimental tests, as shown in Fig. 4.1, *Electric-Fuel C1-33* zinc-air cells and *Sony 18650* lithium-ion cells were use to build the hybrid.

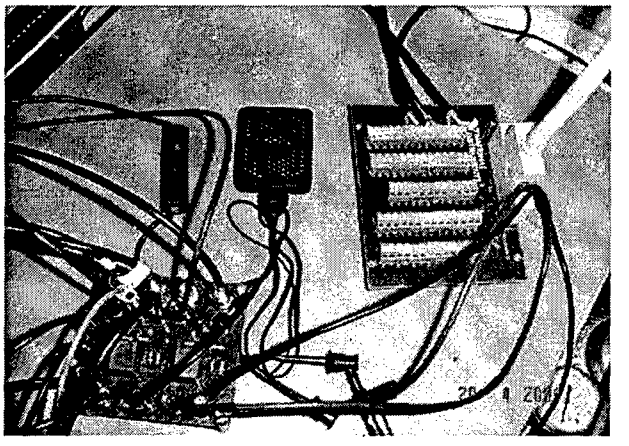

Fig. 4.1. Experimental setup for hybrid battery system

The hybrid system was then compared with the lithium-ion battery alone to determine the battery life until the system attains the cut-off voltage (2.5V). The histogram in Fig. 4.2 shows the lifetime per gram of the batteries at various duty ratios of the pulsed load. The data show that when the duty ratio of the pulsed load varies from 5% to 20% (the normal operating range for short-duration pulsed devices), the service life per gram of the hybrid is almost twice that of the lithium-ion battery alone. When the duty ratio varies from 25% to 100% (the normal operating range for long-duration pulse devices), a good service life per gram is obtained from the hybrid. However, it should be noted that these results are obtained when the system is not running in safe operational limits (the maximum current of the individual battery was exceeded). It can be concluded that the lifetime of the hybrid system (at unit weight) increases twofold over the lithium-ion battery for pulse current loads with a small duty ratio (for peak current).

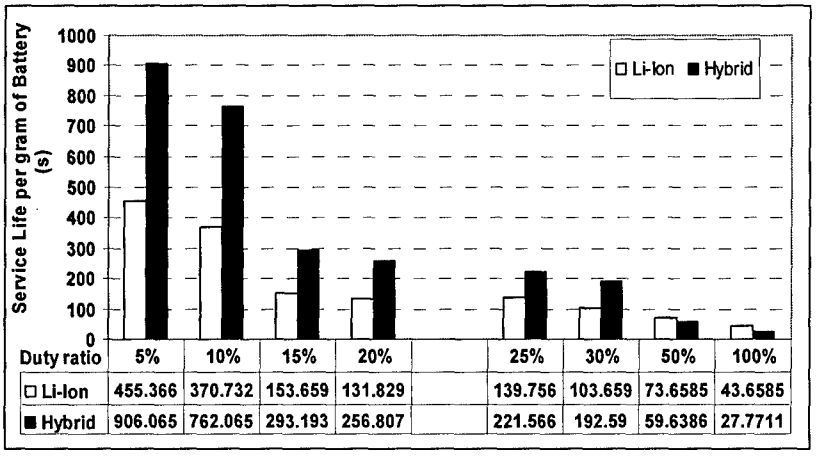

Duty ratio	5%	10%	15%	20%	25%	30%	50%	100%
Li-Ion	455.366	370.732	153.659	131.829	139.756	103.659	73.6585	43.6585
Hybrid	906.065	762.065	293.193	256.807	221.566	192.59	59.6386	27.7711

Fig. 4.2. Comparison of service life per gram of hybrid battery system and lithium-ion alone for various duty ratios.

The hybrid system was further tested to determine the optimum battery size for a given pulse-current load (high current: 1.2A, low current: 0.2A, duty ratio: 20%, period: 600s). The ref-

erence configuration is a single-cell lithium-ion battery in parallel with a three-cell zinc-air battery. The optimal configuration is achieved by varying the lithium-ion battery capacity while keeping the zinc-air battery capacity fixed. Care should be taken so that the currents of the zinc-air battery and the lithium-ion battery stayed under 0.5A and 2.0A respectively. This test was repeated for various duty ratios until the system attained the cut-off voltage (2.5V). Fig. 4.3 shows a histogram that compares the battery life per gram under the pulsed load of different duty ratios for both the optimized and reference configurations. For a low pulse load, the service life per gram of the hybrid increases; this increase can be attributed to a net decrease in system weight, since more zinc-air components are used compared to the lithium-ion component. However, the service life of the hybrid decreases as the duty ratio of the pulsed load increases. Note that the capacity of the lithium-ion battery decreases to an extent where the zinc-air battery current remains below its permissible value (0.5A) and the lithium-ion battery current remains below 2.0A.

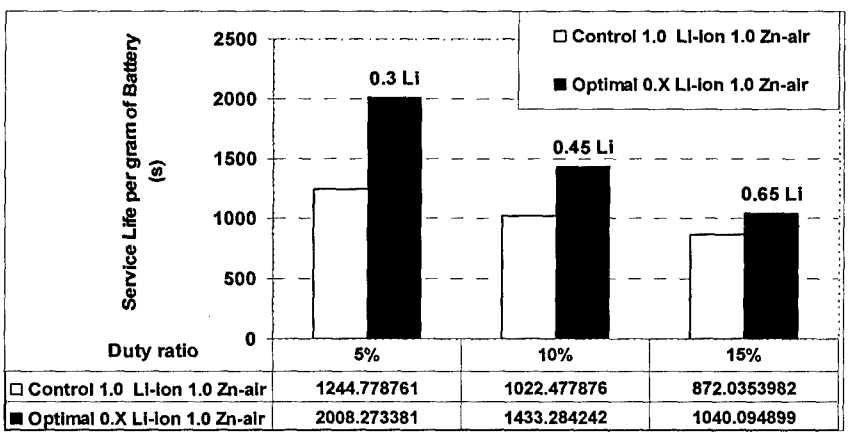

Fig. 4.3. Service life per gram of hybrid battery system as capacity of lithium-ion battery is changed.

FUEL CELL/ BATTERY HYBRID POWER SOURCE

The performance of two configurations of active fuel cell/battery power source hybrids, created by interposing a dc/dc converter between a fuel cell and a battery, were investigated and compared using both theory and experiment with special attention to the peak power enhancement, and power losses in the converter. The two configurations are shown in Fig. 4.4. Configuration (I) and Configuration (II), corresponding to the load connected to node 1 and node 2 respectively. In Configuration (I), the fuel cell is isolated from the large pulse power demands of the load by a converter and the battery supplies the load directly. Configuration (I) uses a current unidirectional power converter and Configuration (II) requires a current bidirectional converter. Fig. 4.5 shows the experiment setup of active controlled fuel cell/battery hybrids.

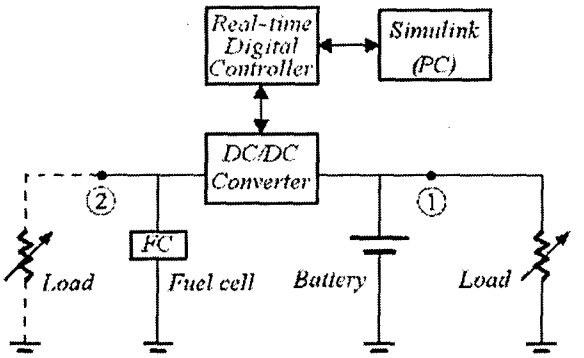

Fig. 4.4. Configurations of the active hybrid power source.

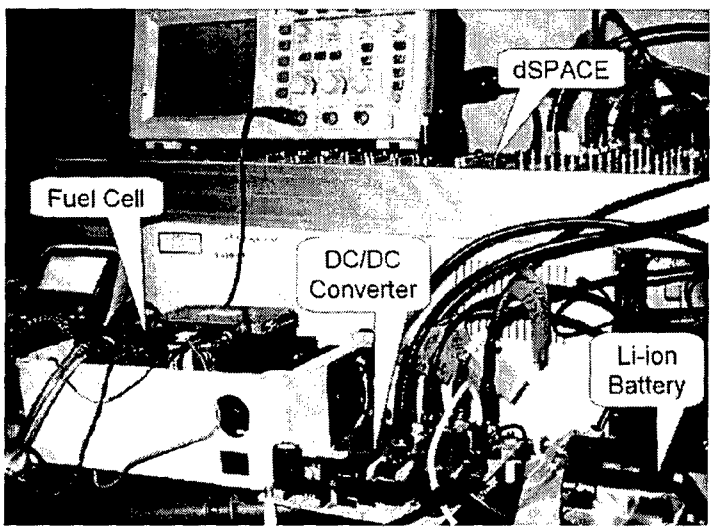

Fig. 4.5. Experiment setup of active controlled fuel cell/battery hybrids.

Both of the defined configurations were built, using a 35 W polymer electrolyte membrane (PEM) fuel cell, an 8-cell lithium-ion battery pack, and a high-efficiency power converter. Both configurations yielded a peak power output of 135 W, about 4 times as high as the fuel cell alone could supply, with only a slight (13%) increase of weight. Which of the two configurations yields a smaller loss depends on the load power demand characteristics including peak power and load duty ratio.

An adaptive control strategy of the power converter for active battery/ fuel cell hybrid power source was investigated by simulation and experiments, as shown in Fig. 4.6. This control strategy can adjust the output current set point of the fuel cell according to the state-of-charge (or voltage) of the battery and appropriately distribute the electrical power between the fuel cell and the battery. It is applicable in two topologies of active fuel cell/battery hybrids.

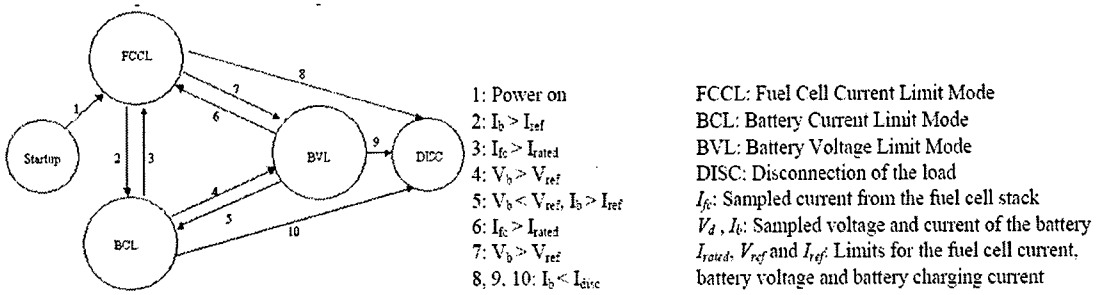

Fig. 4.6. State machine representation of control strategy for fuel cell-regulated/battery-floating configuration.

BATTERY/ULTRACAPACITOR HYBRID POWER SOURCE

The performance of an actively controlled battery/ultracapacitor hybrid, as shown in Fig. 4.7, was investigated by simulation and experimental tests in terms of power enhancement, discharge cycle life, specific power, and energy loss with respect to pulse load profiles. A DC-DC converter was used to actively control the power flow from a battery, to couple the battery to an ultracapacitor for power enhancement, and to deliver the power to a load efficiently. Fig. 4.8 shows a photograph of the experimental setup.

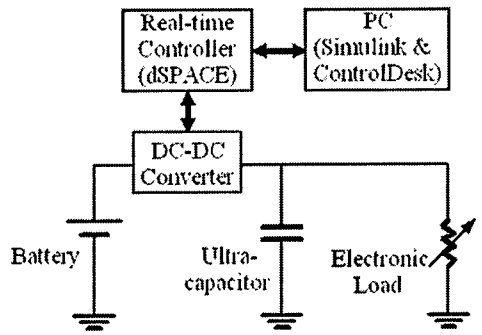

Fig. 4.7. The actively controlled battery/ ultracapacitor hybrid.

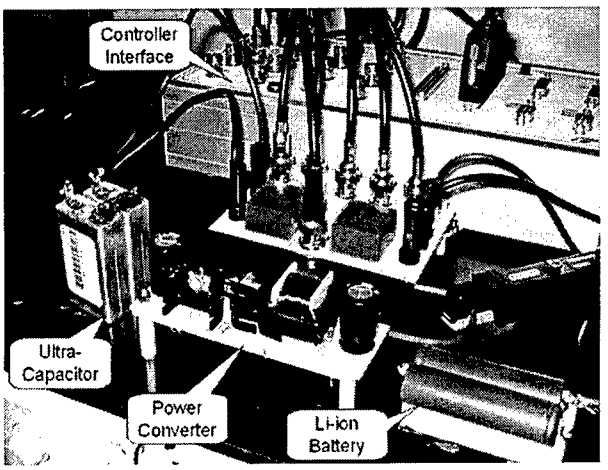

Fig. 4.8. Experimental setup of the active hybrid system.

The experimental data in comparison to the simulation results are shown in Fig. 4.9 for the battery current, ultracapacitor voltage, and converter output power, respectively. The agreement between the simulation and the experimental results successfully validated both the experimental design of the hybrid system and the simulation models of the system.

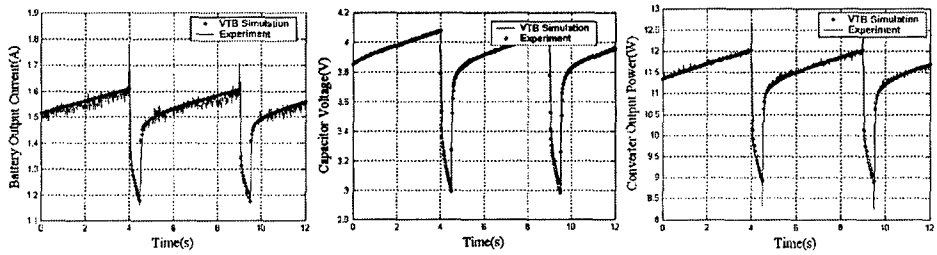

Fig. 4.9. Comparison of the simulated and experimental battery current, ultracapacitor voltage, converter output power.

A specific example of the hybrid built from two size 18650 lithium-ion cells and two 100 F ultracapacitors achieved a peak power of 132W which is a three-times improvement in peak power compared to the passive hybrid power source (hybrid without a converter), and a seven times improvement as compared to the lithium-ion cells alone. Furthermore, the operation of an active hybrid results in a much lower battery current with very small ripples, and therefore a lower battery temperature, which are preferred by many applications for a longer battery lifetime. The discharge cycle time is reduced for the active hybrid due to an added converter loss and increased ultracapacitor loss. A compromise should be made between the power enhancement and the discharge cycle time in order to achieve optimized results depending upon applications. The design can be scaled to larger or smaller power capacities for various applications.

A battery/ultracapacitor hybrid power source with a current-mode control loop, as shown in Fig. 4.10, for a pulsed load operation was designed and analyzed. The hybrid has the advantages of highly enhanced power and better cycle life characteristics compared to a battery-alone system. The power ~ efficiency relation derived from the steady-state analysis allows to predict and optimize the system power and efficiency performances. The small-signal analysis yields a closed-loop control system with a simple proportional compensator that can greatly improve the transient characteristics and steady-state accuracy, and in the meanwhile eliminate potential instabilities induced by the high resistance mode of the battery.

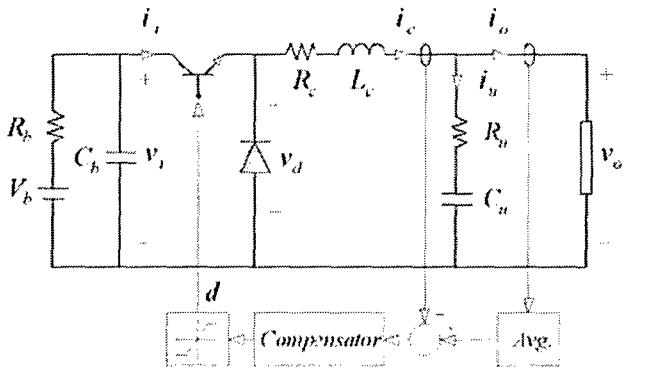

Fig. 4.10. The battery/ultracapacitor hybrid with a current-mode control loop.

EFFICACY OF FUEL-CELL POWERED BATTERY CHARGERS

Two control strategies for active power sharing in a fuel cell powered battery charging station were investigated by simulation and experiments. The system diagram is shown in Fig. 4.11. The first one was the real-time strategy. This control scheme adjust the charging currents of the batteries being simultaneously charged in real-time according to the estimated state-of-charge (SOC) which is obtained by estimating the battery open-circuit voltage with current correction and linearly fitting between the open-circuit voltage and the state-of-charge.

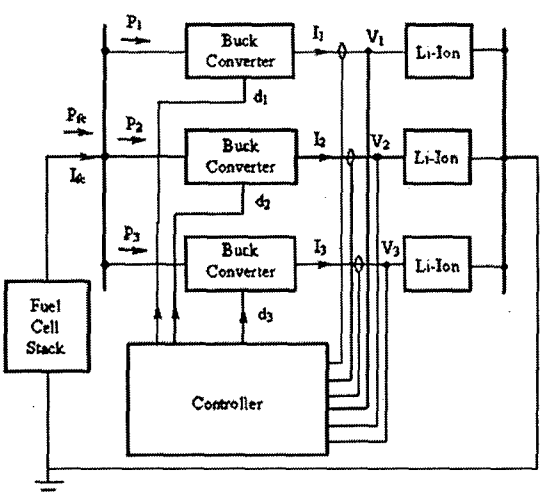

Fig. 4.11. Block diagram of the fuel-cell-powered battery-charging station.

The measured battery voltages and charging currents are shown in Fig. 4.12, where the simulated voltages and currents under the same initial conditions are also plotted. From Fig. 4.12, it is seen that during current regulation mode the battery voltages were different and the charging currents varied with the voltage in real-time. The battery with the lowest initial voltage (and thus the least initial charge) was charged with the highest current, and its voltage increased more rapidly than the others. This feature implies that real time charging strategy can help to reduce the

total charging time. The voltages of these batteries reached the reference voltage almost simultaneously and then their currents tapered. It is shown that all of three batteries became fully charged almost simultaneously. From the experiment results, it is also seen that the proposed method for battery state-of-charge estimation was effective for the active power sharing strategy.

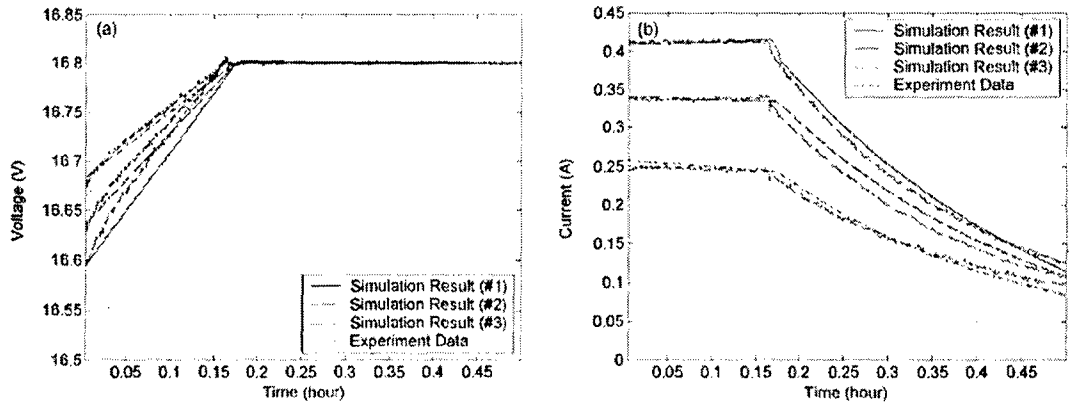

Fig. 4.12. The measured battery voltages and charging currents: (a) voltages, (b) currents. (a) From top to down (on the left vertical axis): voltages of batteries #3, #2, #1 (b) from top to down: charging currents for batteries #1, #2, and #3.

The second one was the synergetic controller for pulse current charging of advanced batteries from a fuel cell power source. This control approach was applied to regulate the buck converters that control the pulse charging currents to the many batteries. Fig. 4.13 shows the system schematic in the VTB environment. The dynamic characteristics of the synergetic controller were studied and compared with PI controller by conducting system simulation and experimental tests. Experiment results, as shown in Fig. 4.14 validate that the synergetic controller is less sensitive to the parameter variation and input variation and is robust to the pulse output change. The synergetic controller achieves better performances than the linear regulators. Experiment studies also show that the efficiency of the whole system is greater than 90% and the total charging time for three batteries with pulse current charging protocol is about 25% shorter than that with dc charging protocol.

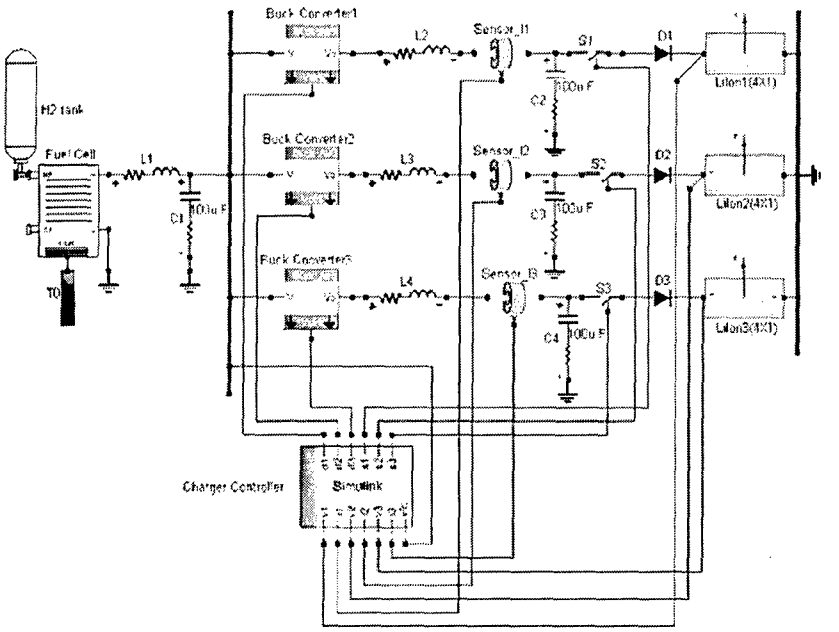

Fig.4.13. Virtual prototype of the fuel cell powered battery-charging station in the VTB environment.

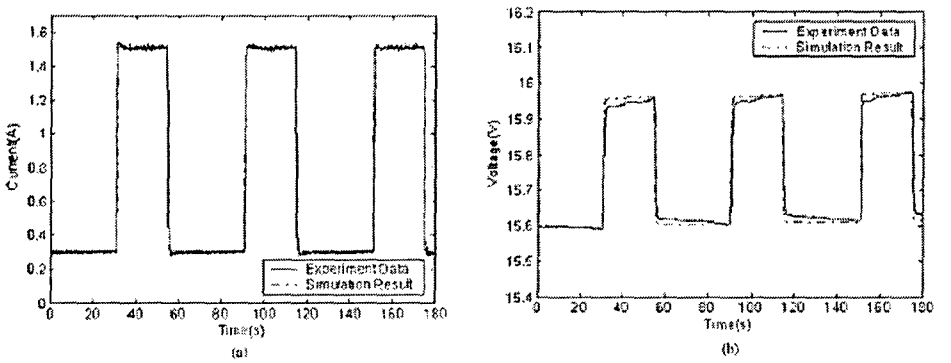

Fig. 4.14. Experimental data and simulation results of the charging current and voltage of a single battery with the synergetic controller: (a) current and (b) voltage.

EXERGY MINIMIZATION

USE OF SECONDARY CELLS AS TEMPORARY ENERGY REPOSITORIES

Energy reclamation from partially depleted primary batteries, using secondary battery cells as temporary energy repositories, was studied using pre-validated battery models. A DC/DC power converter was interposed between the two types of batteries to control the discharging of the primary battery and the charging of the secondary battery.

A simple application scenario is used to show the potentially significant benefit of performing this energy reclamation. Fig. 5.1 schematically illustrates the battery energy-reclamation system in the VTB, in which a $LiSO_2$ primary battery is chosen as the partially depleted battery

and a Li-ion battery pack is used as the temporary energy repository. A DC/DC step-down power converter is interposed between these two batteries and it is commanded by a PI controller to discharge the partially depleted primary battery and simultaneously charge the secondary batteries.

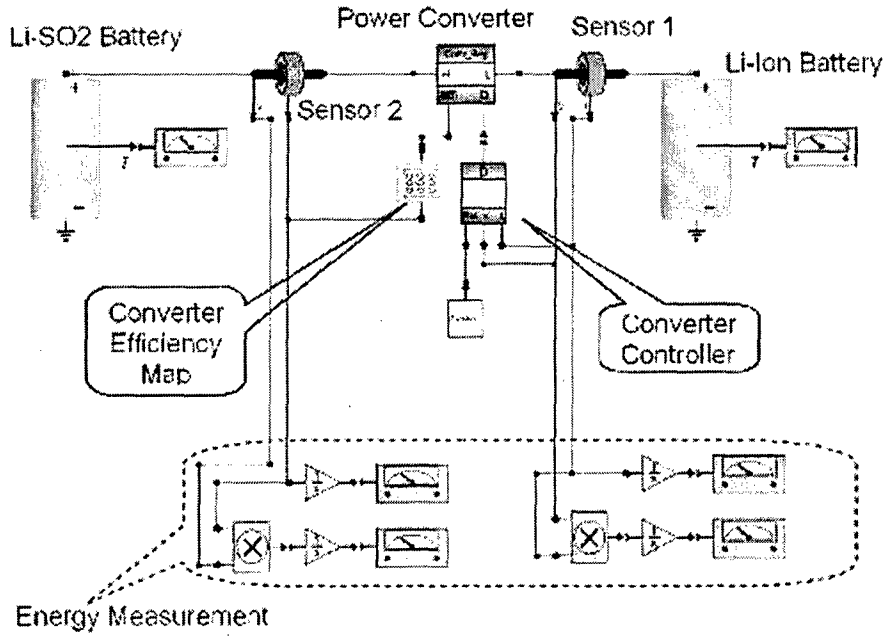

Fig. 5.1. System simulation Schematic in VTB.

For the $LiSO_2$ battery (Saft BA-5590, 15V15Ah) model used in this study, battery features of the rate-dependent and the temperature-dependent characteristics are illustrated in Figs. 5.2 and 5.3, respectively. Fig. 5.2 shows the battery terminal voltage as the function of the depth of discharge at 293 K at different discharging currents from 1.0 A to 8.0 A. Fig. 5.3 illustrates the battery discharging capacity as the function of the discharging current at different temperatures from 233 K to 328 K.

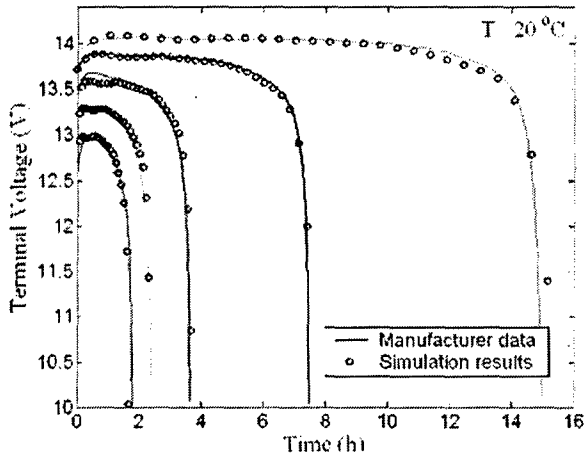

Fig. 5.2. Terminal voltages vs. discharge time, at discharging currents (top to bottom) 1A, 2A, 4A, 6A, and 8A.

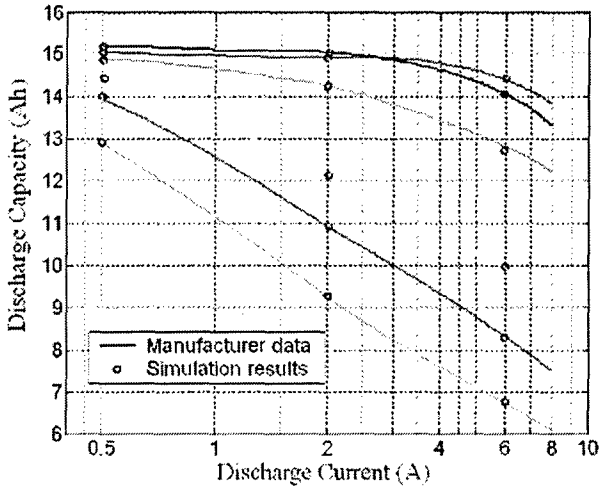

Fig. 5.3. Discharge capacity vs. discharge current, at temperatures of (top to bottom) 328K, 293K, 273K, 253K, 243 K and 233K.

For an example system including a lithium sulfur dioxide primary battery with an initial state-of-charge of 0.3 at 296 K, an aggregated total of 216 KJ of energy is reclaimed and 83% of the energy (179 KJ) is stored in a 10-cell lithium-ion battery pack. The study results demonstrate that 8.3% of weight and 10% of cost are saved. The study results also show that appropriate increase of the ambient temperature, using relatively low discharging current, and improving the power converter efficiency at the user-specified current rate can increase battery energy reclamation.

DESIGN AN AUTOMATIC ENERGY OPTIMIZATION CAPABILITY

A system for automatic recovery and consolidation of energy from partially spent batteries, as shown in Fig. 5.4, was designed and analyzed using numerical simulation in the VTB. The

objective for this system was to minimize the stockpile of batteries needed to run a suite of portable electronic devices on a daily, mission-oriented, basis. This system is adapted to various battery types and allows the user to conveniently choose between charging and discharging specific batteries without changing the battery positions. The control algorithm, as shown in Fig. 5.5, was able to automatically select which secondary batteries should preferentially be charged. The control algorithm also continuously adjusted the discharging current of each battery according to its estimated state-of-charge.

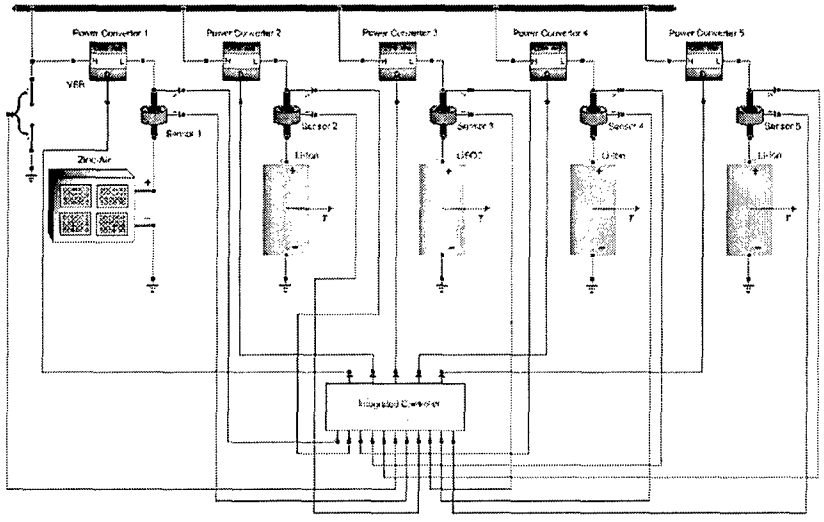

Fig. 5.4. VTB schematic of automatic energy recovery system for partially spent batteries.

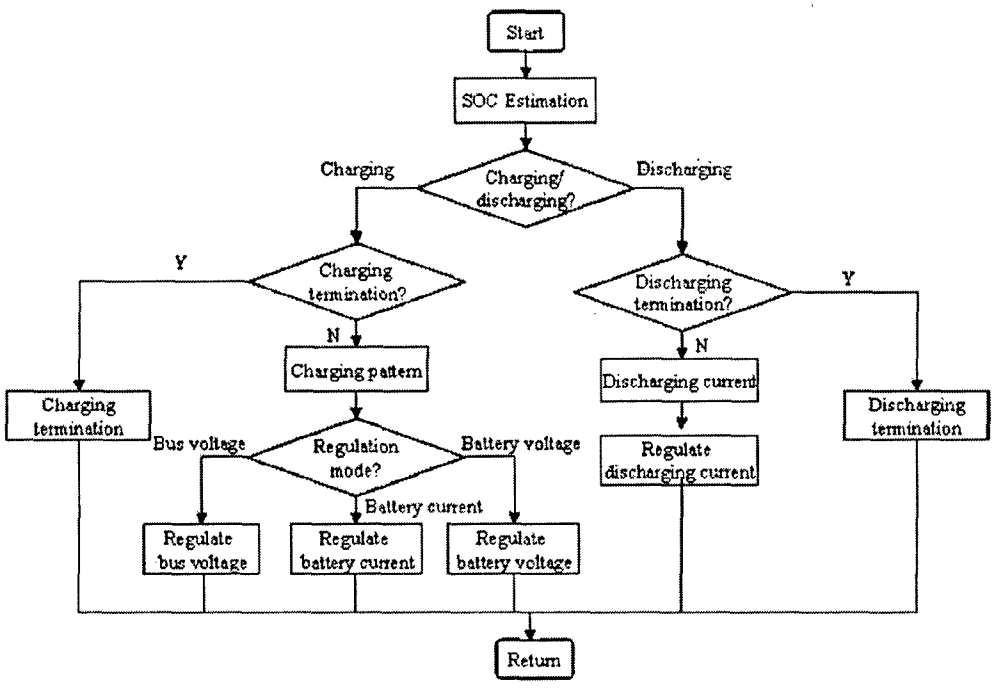

Fig. 5.5. Flow chart of control algorithm.

PHOTOVOLTAIC POWER SOURCES

MAXIMUM POWER TRACKING IN SOLAR ARRAYS

Photovoltaic energy conversion offers a mechanism for providing renewable on-site power without any need to transport fuels. Partial shading of the solar array, a persistent problem in portable applications, was addressed in some detail here. A state space approach to the design of a maximum power point (MPP) tracking system for photovoltaic energy conversion was presented. The problem of optimal-power control of a nonlinear time-varying system is reduced to an ordinary problem of dynamic system stability in state space by applying MPP conditions in controller design. The resulting tracking system searches for the reference point and tunes the converter for maximum power delivery to a load that may represent an end-user, or an energy-storage element, or a power grid-interface.

The proposed design procedure for the MPP tracking system ensures a global asymptotic stability under certain conditions, and a minimum degree of the dynamic feedback. The tracking accuracy of the controller depended solely on accuracy of computation of the necessary derivatives of the reference point with respect to time. It has also been shown that the proposed controller yields a stable closed loop system capable of tracking the maximum power point with desired accuracy. To demonstrate effectiveness of the proposed approach to the partially shaded PV module control, the system presented in Fig. 6.1 was considered and validated in the VTB simulation environment. As can be seen, the system in Fig. 6.1 consists of two arrays, connected in parallel, but one array receives direct sunlight, while the other one is shaded.

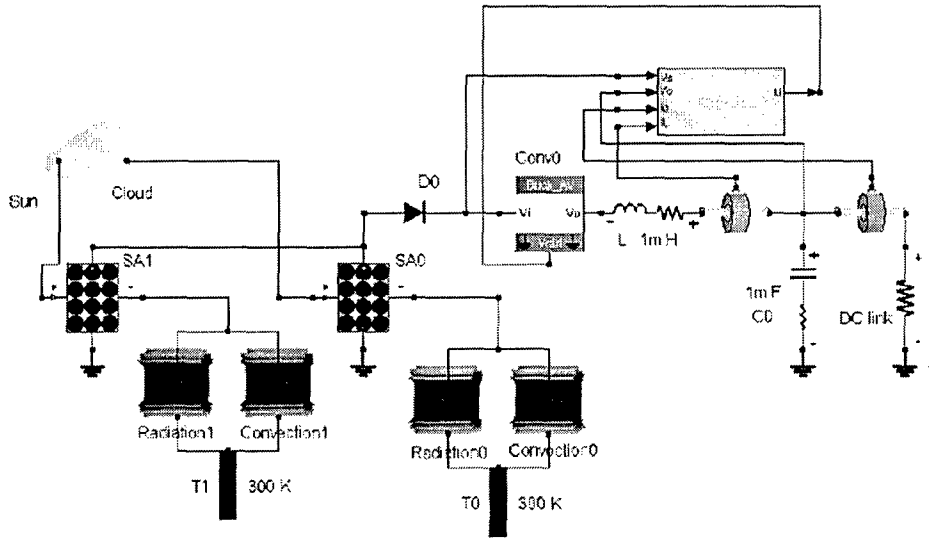

Fig. 6.1. A partially shaded solar array MPP tracking system in the VTB environment.

The results of simulation of the partially shaded solar array system that employs the proposed control algorithm are shown in Fig. 6.2. Fig. 6.2 presents a comparison between the total maximum possible power of the arrays and the actual total power produced by the arrays. As can be seen, both of these curves are in good agreement, and therefore the proposed system effectively tracks the MPP even though the PV module is partially shaded.

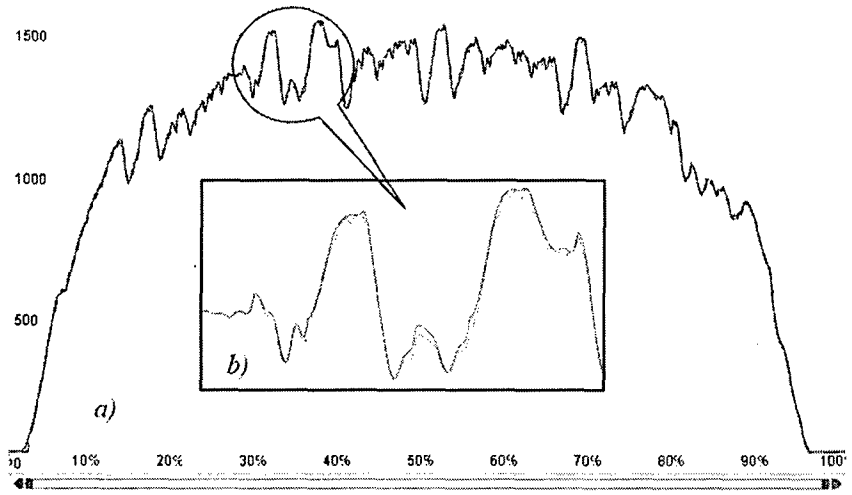

Fig. 6.2. The instantaneous theoretical MPP (solid line) and the power realized (dotdashed line) from the solar array. a) The result for an entire day. b) The zoomed-in region for part of the day.

Optimum Configuration of Solar Array for Enhanced Power Generation

A configuration of cell connections that maximizes the power generated by a solar array was proposed and validated, as shown in Fig. 6.3. The new configuration capitalizes on the prolific growth of low voltage, high current power converters to support the computer industry. Fig. 6.4 shows the prototype of solar panel using optimum configuration and its power converter. The study results demonstrated that, under the complex irradiance conditions typically experienced in portable applications such as for solar arrays embedded inbackpacks or jackets, the power generation capability of the solar array using the proposed configuration is enhanced by a factor of 2 without extra component costs compared to the traditional configuration. In addition, the maximum power point tracking is simplified to a constant voltage control problem, which in turn reduces the complexity of hardware implementation and ensures the control stability.

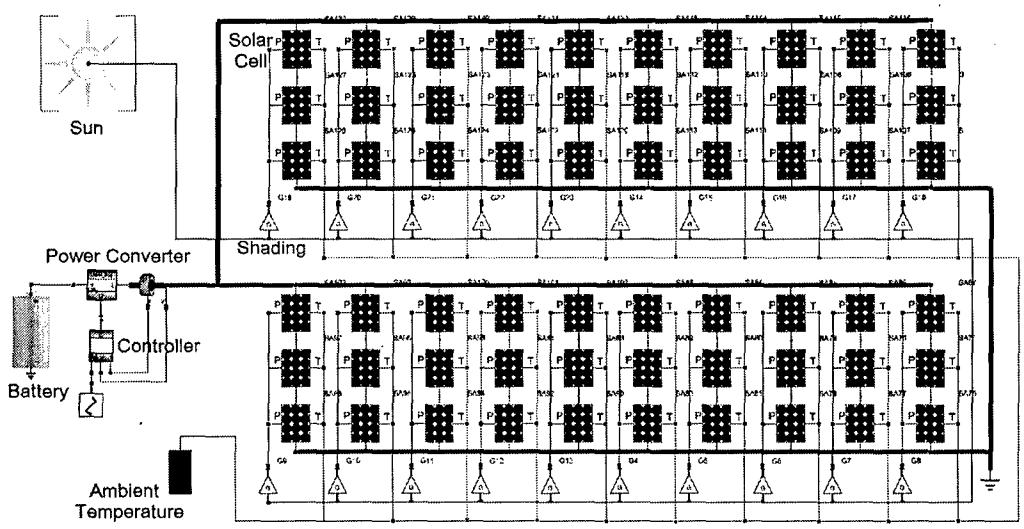

Fig. 6.3 Solar panel connected with an optimum configuration.

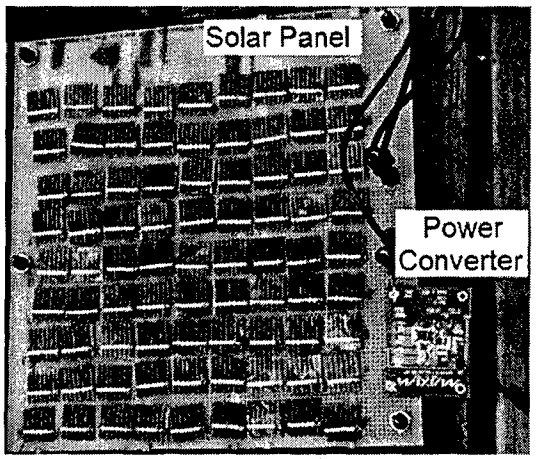

Fig. 6.4. Prototype of solar panel using optimum configuration and its power converter.

DELIVERABLES

The final report and the CD of software are provided as deliverables. The CD contains:

EXECUTABLE VERSION OF THE VTB SOFTWARE

Two versions of VTB software are available on the CD. They are the VTB 2003 and the VTB Pro.

COMPONENT MODELS

The following models have been developed in both the VTB 2003 and the VTB Pro. Full descriptions of these models are available in their model help files for VTB 2003 and related publications provided in Appendices I and II.

Model	Description	VTB2003	VTBPro
BA5590	$LiSO_2$ battery type	Y	Y
BA5800	$LiSO_2$ battery type	Y	Y
BA5390	$LiMnO_2$ battery type	Y	Y
AA	Alkaline battery type	Y	Y
AAA	Alkaline battery type	Y	Y
Sony18650	Li-Ion battery type	Y	Y
PEM	Polymer Electrolyte Membrane fuel cell	Y	Y
DMFC	Direct Methanol Fuel Cell	Y	N
Programmable load	Link to Excel spread sheets to represent different pieces of soldier system equipment	Y	Y

TEMPLATES FOR, AND EXAMPLES OF, MISSION DEFINITION SPREADSHEETS

A Probabilistic Load Profile Generator has been developed and implemented in MS Excel, and it can be accessed through VTB using the Advanced Programmable Load model. The program uses a probabilistic algorithm to generate unique load profiles for a set of items each time the program is executed. The items in the set are defined individually, with each item having its own set of operating modes. Help file of the Probabilistic Load Profile Generator is provided in Appendix II.

VTB SIMULATION TOOL – BATTERY ANALYZER FOR SQUAD LEVEL MISSION PLANNING

The tool is used to maximize energy available to each member of a squad without increasing the total battery count that has to be carried. It has considered equipment and power requirements during the various missions and associated operational environments. Help file of using the simulation tool is provided in Appendix II.

PUBLICATION LIST

JOURNALS

1. S. Liu, R. Dougal and E. Solodovnik, "Design of an Autonomous Photovoltaic Power Plant for Telecommunication Relay Station", IEE Proceedings of Generation, Transmission, and Distribution, Vol. 152, No. 6, pp. 745-754, Nov. 2005.
2. Z. Jiang, R. Dougal, S. Liu, S. Gadre, A. Ebner, J. Ritter, "Simulation of Thermally Coupled Metal Hydride Hydrogen Storage and Fuel Cell Systems", Journal of Power Sources, Vol. 142, Issues 1-2, pp. 92-102, March 2005.
3. Z. Jiang, R. Dougal, "Real-Time Strategy for Active Power Sharing in a Fuel Cell Powered Battery Charger", Journal of Power Sources, Vol. 142, Issues 1-2, pp. 253-263, March 2005.
4. R. A. Dougal, Z. Jiang and L. Gao, "Analysis of an Automatic Energy Recovery System for Partially Spent Batteries", Journal of Power sources, vol. 140, Issue 2, pp. 400-408, Feb. 2005.
5. R. A. Dougal, L. Gao and Z. Jiang, "Effectiveness Analysis of Energy Reclamation from Partially Depleted Batteries", Journal of Power Sources, vol. 140, Issue 2, pp.409-415, Feb. 2005.
6. L. Gao, Z. Jiang and R. A. Dougal, "Evaluation of Active Hybrid Fuel Cell/ Battery Power Sources", IEEE Transactions on Aerospace and Electronic Systems, vol. 41, No. 1, pp. 346-355, Jan. 2005.

7. L. Gao, R. A. Dougal and S. Liu, "Power Enhancement of an Actively-Controlled Battery/Ultracapacitor Hybrid", IEEE Transactions on Power Electronics, vol. 20, No. 1, pp. 236-243, Jan. 2005.
8. Z. Jiang, L. Gao and R. A. Dougal, "Flexible Multiobjective Control of Power Converter in Active Hybrid Fuel Cell/Battery Power Sources", IEEE Transactions on Power Electronics, vol. 20, No. 1, pp. 244-253, Jan. 2005.
9. S. Liu, R. Dougal, E. Solodovnik, "Maximum Power Tracking and Pulse-Width-Modulated Shunt for Satellite Power Systems", AIAA Journal of Propuslion and Power, Vol. 20, No. 5, pp. 911-918, Sep.-Oct., 2004.
10. S. Liu, R. Dougal, E. Solodovnik, "VTB-Based Design of a Standalone Photovoltaic Power System", International Journal of Green Energy, Vol. 1, No. 3, pp. 279-300, Sep.2004.
11. E. Solodovnik, S. Liu, R. Dougal, "Power Controller Design for Maximum Power Tracking in Solar Installations", IEEE Transactions on Power Electronics, Vol. 19, No. 5, pp.1295-1304, Sep. 2004.
12. Z. Jiang, R. Dougal, "Synergetic Control of Power Converters for Pulse Current Charging of Advanced Batteries from a Fuel Cell Power Source", IEEE Trans on Power Electronics, Vol. 19, No 4, pp 1140-1150, July 2004.
13. L. Gao, Z. Jiang and R. A. Dougal, "An Actively Controlled Fuel Cell/Battery Hybrid to meet Pulsed Power Demands", Journal of Power Sources, vol. 130, issues 1-2, pp. 202-207, May 2004.
14. Z. Jiang , L. Gao, M. Blackwelder and R. A. Dougal, "Design and Experimental Tests of Control Strategies for Active Hybrid Fuel Cell/ Battery Power Sources", Journal of Power Sources, vol. 130, Issues 1-2, pp. 163-171, May 2004.
15. Z. Jiang, R. Dougal, "Control Strategies for Active Power Sharing in a Novel Fuel-Cell-Powered Battery-Charging Station", IEEE Transactions on Industry Applications, Vol. 40, No. 3, pp. 917-924, May-June 2004.
16. Z. Jiang, L. Gao and R. A. Dougal, "Adaptive Control Strategy for Active Power Sharing in Hybrid Fuel Cell/Battery Power Sources", accepted by IEEE Transactions on Energy Conversion on March 2005.

PROCEEDINGS

17. Z. Jiang, R. A. Dougal, "A Hybrid Fuel Cell Power Supply with Rapid Dynamic Response and High Peak-Power Capacity", IEEE Applied Power Electronics conference (APEC 2006), pp. 1250-1255, Dallas, TX, March 2006.
18. Z. Jiang, R. A. Dougal, R. Leonard, H. Figueroa, A. Monti, "Hardware-in-the-Loop Testing of Digital Power Controllers", IEEE Applied Power Electronics Conference (APEC 2006), pp. 901-906, Dallas, TX, March 2006.
19. Z. Jiang, R. Dougal, "A Novel Digitally-Controlled, Portable Photovoltaic Power Source", IEEE Applied Power Electronics Conference, pp. 1797-1802, Austin, TX, Mar. 2005.
20. Z. Jiang, Dougal R., Leonard R., "A Novel Digital Power Controller for Fuel Cell/Battery Hybrid Power Sources", IEEE Applied Power Electronics Conference, pp. 467-473, Austin, TX, Mar. 2005.
21. L. Gao, Y. Song and R. Dougal, "Wavelet Neural Network based Battery State-of-Charge Estimation for Portable Electronics Applications", Proc. of the IEEE Applied Power Electronics Conference and Exposition (APEC 2005), Austin, TX, pp. 927-932, Mar. 2005.
22. S. Liu, R. Dougal, Design and Analysis of a Current-Mode Controlled Battery/Ultracapacitor Hybrid, IEEE 39th Industry Applications Society Annual Meeting, pp. 1140-1145, Seattle, WA, Oct. 2004.

23. Z. Jiang, R. Dougal, "Multiobjective MPPT/Charging Controller for Standalone PV Power Systems under Different Insolation and Load Conditions", Proceedings of IEEE Industry Applications Society 39th Annual Meeting, pp. 1154-1160, Seattle, WA, Oct. 3-7, 2004.
24. Z. Jiang, R. Leonard, R. Dougal, H. Figueroa, A. Monti, "Processor-in-the-Loop Simulation, Real-Time Hardware-in-the-Loop Testing, and Hardware Validation of a Digitally-Controlled, Fuel-Cell Powered Battery-Charging Station", 2004 IEEE Power Electronics Specialists Conference, pp. 2251-2257, Aachen, Germany, June 20-25, 2004.
25. Z. Jiang, L. Gao and R. A. Dougal, "Multi-Objective Control of Power Converter in Active Hybrid Fuel Cell/Battery Power Sources", Proc. of the 35th IEEE Power Electronics Specialists Conference (PESC), pp. 3804-3811, Jun. 20-25, 2004, Aachen, Germany.
26. L. Gao, Z. Jiang and R. A. Dougal, "Performance of Power Converters in Hybrid Fuel Cell/ Battery Power Sources", Proc. of the 35th IEEE Power Electronics Specialists Conference (PESC), pp. 2108-2022, Jun. 20-25, 2004, Aachen, Germany.

INVENTION DISCLOSURE

27. "Novel Solar Array Configuration for Enhanced Power Generation", R. Dougal, L. Gao, S. Liu and A. Iotova, USCRF No. 572, April, 2006.

APPENDICES

APPENDIX I - PUBLICATIONS

APPENDIX II - HELP FILES

A1. Lithium-ion battery model help file
A2. LiSO2Battery_BA5590U15V model help file
A3. LiSO2Battery_BA5800U6V model help file
A4. LiMnO2Battery_BA5390U15V model help file
A5. Alkaline AA battery model help file
A6. Alkaline AAA battery model help file
A7. Generic battery model help file
A8. PEM fuel cell model help file
A9. DMFC model help file
A10. Advanced programmable load help file
A11. Advanced probabilistic load profile generator help file
A12. Battery Analyzer for Squad Level Mission Planning help file

APPENDIX III – EXECUTABLE PROGRAMS

All executable programs will be separately delivered on a CD to the Program Officer in Jan. 2007. This delay is necessary to fit the software distribution into the next regularly scheduled build of the VTB software.

REPORT DOCUMENTATION PAGE

Form Approved
OMB No. 0704-0188

1. REPORT DATE *(DD-MM-YYYY)*	2. REPORT TYPE	3. DATES COVERED *(From - To)*
31-12-2006	Final	31-07-2003 to 15-09-2006

4. TITLE AND SUBTITLE
Soldier System Power Sources

5a. CONTRACT NUMBER
N00014-03-1-0952

5b. GRANT NUMBER

5c. PROGRAM ELEMENT NUMBER

6. AUTHOR(S)
Dougal, Roger A
Gao, Lijun

5d. PROJECT NUMBER

5e. TASK NUMBER

5f. WORK UNIT NUMBER

7. PERFORMING ORGANIZATION NAME(S) AND ADDRESS(ES)
University of South Carolina
Electrical Engineering
301 S. Main Street
Columbia, SC 29208

8. PERFORMING ORGANIZATION REPORT NUMBER

9. SPONSORING/MONITORING AGENCY NAME(S) AND ADDRESS(ES)
Office of Naval Research
100 Alabama Street, SW, Suite 4R15
Atlanta, GA 30303-3104

10. SPONSOR/MONITOR'S ACRONYM(S)

11. SPONSOR/MONITOR'S REPORT NUMBER(S)

12. DISTRIBUTION/AVAILABILITY STATEMENT
unlimited

13. SUPPLEMENTARY NOTES

14. ABSTRACT

This work addressed five key issues related to effective use of electric energy by dismounted troops, working both at the individual level and at the squad level, with the fundamental goal of reducing the total mass of the electric power sources carried by a Marine in the Expeditionary Forces while still meeting all of his electric power demands. To achieve that goal, this work investigated the effectiveness of hybrid power sources composed variously of batteries, fuel cells, and super capacitors, it developed control algorithms for those hybrid power sources, it assessed the value of recovering energy from partially spent primary cells, it developed more-efficient methods of capturing energy from photovoltaic sources, and it developed simulation-based tools for planning the carriage of sufficient electric energy to power specific suites of equipment as necessary to accomplish specific missions.

15. SUBJECT TERMS

16. SECURITY CLASSIFICATION OF:			17. LIMITATION OF ABSTRACT	18. NUMBER OF PAGES	19a. NAME OF RESPONSIBLE PERSON
a. REPORT	b. ABSTRACT	c. THIS PAGE			19b. TELEPHONE NUMBER *(Include area code)*